Liquid Crystals
Publication details, including instructions for authors and subscription information:
http://www.informaworld.com/smpp/title~content=t713926090

Laterally dibenzyloxy-branched nematogens with large nematic range and rich solid polymorphism

Cecile Canlet; Bing M. Fung; Frederick Roussel; Karine Leblanc; Philippe Berdague; Jean-Pierre Bayle

Online publication date: 06 August 2010

To cite this Article Canlet, Cecile , Fung, Bing M. , Roussel, Frederick , Leblanc, Karine , Berdague, Philippe and Bayle, Jean-Pierre(2000) 'Laterally dibenzyloxy-branched nematogens with large nematic range and rich solid polymorphism', Liquid Crystals, 27: 5, 635 — 641
To link to this Article: DOI: 10.1080/026782900202480
URL: http://dx.doi.org/10.1080/026782900202480

LIQUID CRYSTALS, 2000, VOL. 27, NO. 5, 635–641

Laterally dibenzyloxy-branched nematogens with large nematic range and rich solid polymorphism

CÉCILE CANLET, BING M. FUNG
Department of Chemistry and Biochemistry, University of Oklahoma, Norman, Oklahoma 73019-0370, USA

FRÉDÉRICK ROUSSEL
Laboratoire de Dynamique et Structure des Matériaux Moléculaires, Université du Littoral, U.R.A. 801, MREID, 59140 Dunkerque, France

KARINE LEBLANC, PHILIPPE BERDAGUÉ and JEAN-PIERRE BAYLE*
Laboratoire de Chimie Structurale Organique, Université Paris XI, U.R.A. 1384, 91405 Orsay Cedex, France

(*Received 17 September 1999; accepted 19 November 1999*)

Mesogenic compounds containing four rings in the core usually have very high melting points. However, when two identical lateral benzyloxy groups are introduced on the same side of one of the central rings, the melting point is lowered dramatically and a large nematic range is retained. This range is affected by the bulkiness of the *para*-substituents in the lateral rings. Methyl groups can be introduced in the *ortho*- or *meta*-positions with a consequent decrease in the melting temperature without much affecting the nematic range. These compounds exhibit a rich solid polymorphism which is certainly related to the effect of the conformations of the lateral substituent on the molecular arrangment in the solid phase. Some preliminary NMR experiments on the nematic phase indicate that the molecular long axis coincides with the core axis, whereas the *para*-axis of the lateral fragment makes an angle close to the magic angle with respect to the molecular long axis.

1. Introduction

Lateral substituents normally cause a depression in the transition temperatures of a mesogen. Usually the clearing temperature is depressed more than the melting temperature, leading for large lateral substituents to a loss of the mesophase [1–4]. This deleterius effect can be counterbalanced by increasing the molecular anisotropy and consequently decreasing the influence of the lateral substituent [5–7] or by letting lateral aromatic substituents come closer together through π–π interactions in order to obtain more or less calamitic molecules [8]. The first approach used by several groups [9–13] will be developed in the following text. For example, if we consider a lateral alkoxy chain introduced in the middle part of the molecule, compounds with two rings in the main core do not present any mesomorphic properties, whereas compounds with three rings may have some liquid crystalline properties, and adding a fourth ring in the main core enlarges the mesomorphic range considerably. The position of the lateral substituent is of considerable importance. It has been noted that the flexible lateral substituent has to be aligned along the core in the mesophase [14–16] in order to attain a large mesomorphic range. There are two key points about this: the rigidness of the fragment on which the substituent is attached and the position of the substituent which should be as near as possible to the molecular centre. Under these conditions, the nematic phase is preferred as the lateral substituents overlap the core preventing the core-chain segregation.

* Author for correspondence; e-mail: jpbayle@icmo.u-psud.fr

Liquid Crystals ISSN 0267-8292 print/ISSN 1366-5855 online © 2000 Taylor & Francis Ltd
http://www.tandf.co.uk/journals

We have shown recently that one lateral substituent bulkier than an aliphatic chain can be introduced in the molecule without destroying the liquid crystalline properties [17]. In these compounds a lateral chain and a nearby aromatic ring were introduced as shown below:

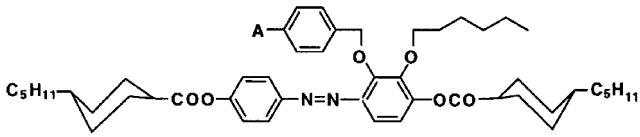

4-A-C6COO

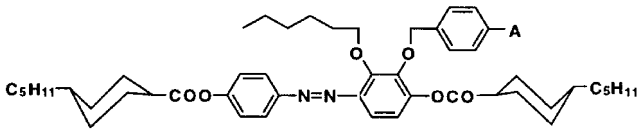

4-A-C6NN

Further replacement of the lateral chain by another lateral ring is of interest as this is expected to increase the anisotropic shape of the molecule leading possibly to the attainment of biaxial nematics [18]. In this paper, we present the synthesis, the mesomorphic properties, and some ^{13}C NMR spectra of new dilaterally substituted compounds containing two bulky lateral aromatic rings whose shapes are far from the conventional rod-like shape. These compounds contain the same four-ring system as in the above structures: two aromatic rings in the middle part of the molecule and two alicyclic rings at the ends. In one of the inner aromatic rings, two equivalent lateral benzyloxy groups are introduced. The compounds differ in the types and positions of the substituents on the lateral aromatic branches (R_1, R_2, R_3 = H, Cl, F, CH_3, C_2H_5, $CH(CH_3)_2$, $C(CH_3)_3$):

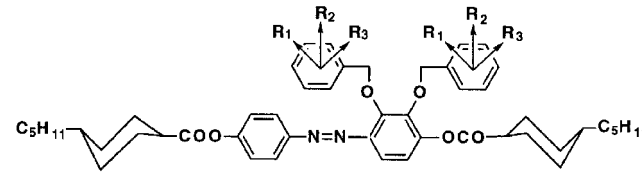

The compounds are labelled following the type of substitution on the two equivalent lateral aromatic branches. For example, compound **4-Cl** (figure 1) has one chlorine in the *para*-position with respect to the $-CH_2-O-$ link on each aromatic branch.

2. Experimental

2.1. *Synthesis*

The compound **4-Cl** was prepared according to the scheme shown in figure 1; other compounds were synthesized using similar procedures.

The above procedure is similar to one already published [17], with the exception of the preparation of 2,3-di-(4-chlorobenzyloxy)phenol. Thus, we will give only the detailed procedure for this compound. 1 eq of 1,2,3-trihydroxybenzene (THB) and 2.5 eq of sodium hydroxide were dissolved in a mixture of PEG200/dioxan (40/60) under nitrogen at 100°C. 2 eq of 4-chlorobenzyl bromide dissolved in the same solvent mixture were added slowly, and the resulting mixture was kept at 100°C for 24 h. Then, the dioxen was evaporated, water was added, and the mixture was acidified. After three extractions with ether, the resulting ethereal phase

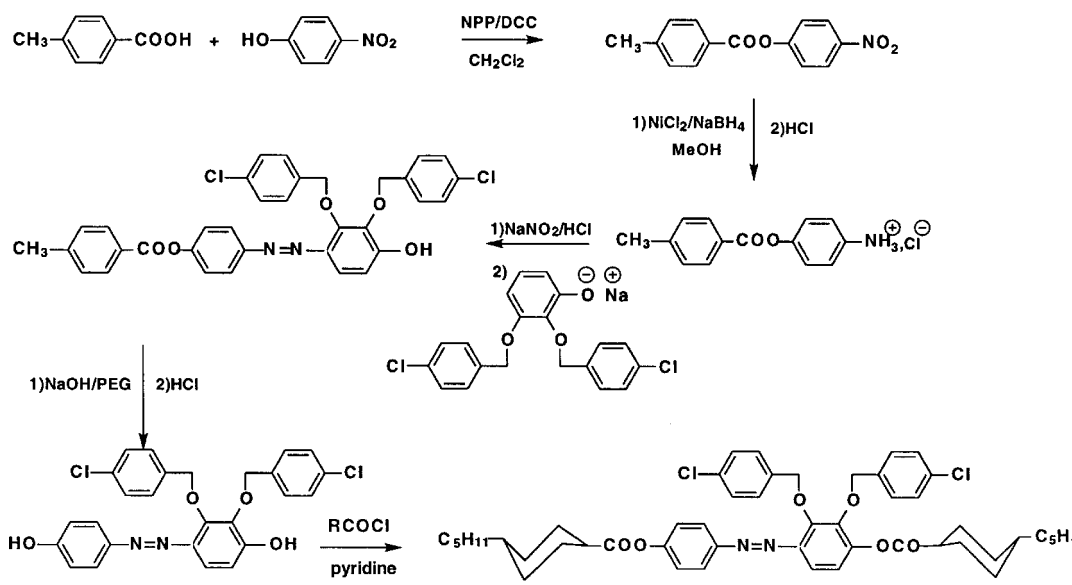

Figure 1. Synthetic scheme for compound **4-Cl**.

was washed several times with 1M aqueous acid to remove the PEG200. After drying and evaporating the solvent, the crude product was chromatographed on silica gel (60–200 mesh) with CH_2Cl_2/heptane (80/20) as eluent, and the disubstituted phenol was collected as the second fraction. The compound collected was pure 2,3-di-(4-chlorobenzyloxy)phenol free from the 2,6-disubstituted isomer.

2.2. *DSC experiments*

The phase transitions were obtained using a Perkin-Elmer DSC7 apparatus and characterized by using a BH2 Olympus polarizing microscope fitted with a PR 600 Linkam heating stage—see the table.

2.3. *NMR experiments*

It will be shown that the pure compounds exhibit solid polymorphism, with a rather drastic change in the density in the solid phase. The change in density during the solid–solid phase transitions caused the NMR tubes to break on cooling or heating the sample. To avoid this problem and to decrease the melting temperature, we chose to mix the compounds studied, **4-CH_3** and **4-$CH(CH_3)_2$**, with ZLI 1167, which is an eutectic mixture of *n*-alkylbicyclohexylcarbonitriles. ZLI 1167 has a negative anisotropic magnetic susceptibility $\Delta\chi$, but contains no aromatic carbons to interfere with the NMR signals in which we are interested. We used samples containing approximately 50 wt % of ZLI 1167 and 50 wt % of our compounds. Under these conditions, the resulting mixture is a liquid crystal at room temperature, has a clearing temperature just below 100°C, and possesses a positive $\Delta\chi$ which leads to the alignment of the director parallel to the magnetic field.

3. Results and discussion

3.1. *Transition temperatures of the unmelted compounds*

The transition temperatures from the first heating cycle (heating rate of 10°C min^{-1}) starting from the unmelted compounds are given in the table.

All the compounds exhibit an enantiotropic nematic phase. Figure 2 provides a comparison of the transition temperatures. Several comments can be made about the data shown in the table and figure 2: (1) The replacement of one lateral ring bearing a terminal methyl group (compound **4-CH_3**) by a hexyloxy chain (compounds **4-CH_3-C6COO** and **4-CH_3-C6NN**) has little effect on the transition temperatures, because the second ring fits into the empty space created by the first one. Thus the packing in the nematic phase is not affected too much

Table. Transition temperatures (in °C) and related entropies for the 10 new compounds. These values are taken with increasing temperature (heating rate 10°C min^{-1}). Two previously published compounds (indicated by *) have been added to the table for comparison. In these compounds, one of the lateral benzyloxy rings is replaced by a hexyloxy chain *ortho*- to the azo bond (**4-CH_3-C6NN**) or *ortho*- to the ester bond (**4-CH_3-C6COO**).

Compound	Cr_1	→ ($\Delta S_{CrCr}/R$)	Cr_2	→ ($\Delta S_{CrN}/R$)	N	→ ($\Delta S_{NI}/R$)	I
H (1)	•	76.5 (9.2)	•	79.5 (1.4)	•	175 (.26)	•
4-CH_3 (2)			•	73.5 (9.1)	•	162.5 (.20)	•
4-CH_3-C6NN(*)			•	55 (44.7)	•	162.5 (1.1)	•
4-CH_3-C6COO(*)			•	74 (35.2)	•	150.5 (.80)	•
4-C_2H_5 (3)	•	72 (4.6)	•	80 (9.1)	•	146.5 (.15)	•
4-$CH(CH_3)_2$ (4)			•	97 (11.1)	•	122 (.11)	•
4-$C(CH_3)_3$ (5)			•	103.5 (11.2)	•	106 (.096)	•
4-F (6)			•	86 (9.3)	•	166 (.17)	•
4-Cl (7)			•	105 (10.5)	•	152.5 (.16)	•
3,5-diCH_3 (8)			•	100 (10.7)	•	152.5 (.16)	•
2,5-diCH_3 (9)			•	70 (8.6)	•	134 (.19)	•
2,4,6-triCH_3 (10)					•	94 (.12)	•

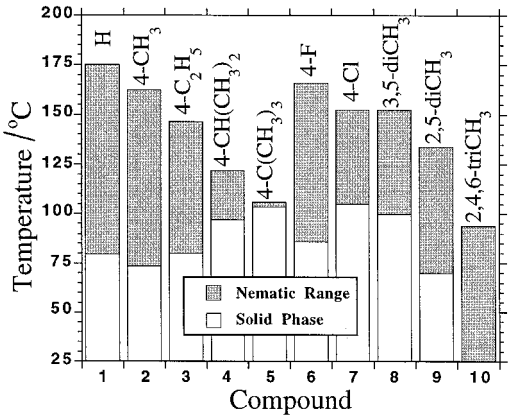

Figure 2. Nematic ranges of the 10 compounds. The transition points were measured by DSC (Perkin-Elmer DSC7) using a heating rate of 10°C min^{-1}.

if there are two lateral rings instead of one lateral ring and one lateral chain. (2) The bulkiness of the substituent in the *para*-position of the lateral ring plays an important role, and the nematic range decreases steadily when the size of the *para*-substituent on both rings changes from hydrogen to a *t*-butyl group. This type of substitution adds to the molecular width, with a consequent increase in the molecular disordering and a reduction in mesophase stability. (3) The replacement of the terminal hydrogen by a fluorine or chlorine atom does not help. Therefore, it seems that the size of the substituent has a major effect, and the lateral dipole does not play a predominant role and has no effect on the phase type. For example, **H** and **4-F** have almost the same transition temperatures, but the nematic range is strongly reduced in **4-Cl**. (4) The introduction of methyl groups away from the C2 axis of the lateral ring noticeably decreases the clearing temperatures. Interestingly, when these methyl groups are introduced pointing towards the centre of the molecule, the melting temperature decreases substantially, yielding a nematic phase at room temperature for **2,4,6-triCH$_3$**. This effect may be related to the decrease of the conformational disordering of the lateral fragment induced by the steric hindrance of these methyl groups. This hindrance may permit a better alignment of the lateral substituents along the core with a consequent reduction in the interactions in the solid phase.

The values of $\Delta S_{NI}/R$ (see the table) have the same order of magnitude as for other laterally disubstituted compounds with an aromatic branch and an alkoxy chain [17]. However, the actual values are slightly smaller than the corresponding values obtained for compounds containing a single lateral chain ($\Delta S_{NI}/R$ typically in the range of 0.5 to 0.8) [15] and in the same range as those for compounds containing two alkoxy chains ($\Delta S_{NI}/R$ typically in the range of 0.15 to 0.2) [6]. It is interesting to note that $\Delta S_{NI}/R$ decreases smoothly from compound 1 to 5, showing again that the bulkiness of the *para*-group on the lateral ring perturbs the stability of the mesophase.

3.2. *Thermal behaviour upon temperature cycling*

All the compounds except **4-C(CH$_3$)$_3$** and **4-Cl** present an interesting behaviour upon temperature cycling. A large difference is seen in the thermograms on increasing the temperature before and after the sample is melted. As an example, we present in figures 3 and 4 the thermal behaviour of the compounds **4-CH(CH$_3$)$_2$**, **4-C$_2$H$_5$** and **H**.

Let us first consider the behaviour of **4-CH(CH$_3$)$_2$** presented in figure 3. During the first heating at 5°C min^{-1}, figure 3 (*a*), the solid–nematic transition appears at 97°C (see the table). After cooling and crystallization of the compound, one new peak appears as a solid–solid transition. More surprisingly, the new melting temperature is 77.5°C, showing a decrease of nearly 20°C in comparison with the temperature obtained in the first run. The clearing temperature on further heating remains the same at 122°C, indicating that no chemical change is involved in the modification of the thermogram. This shows clearly that at least three kinds of structurally different solids can be obtained, depending on the thermal

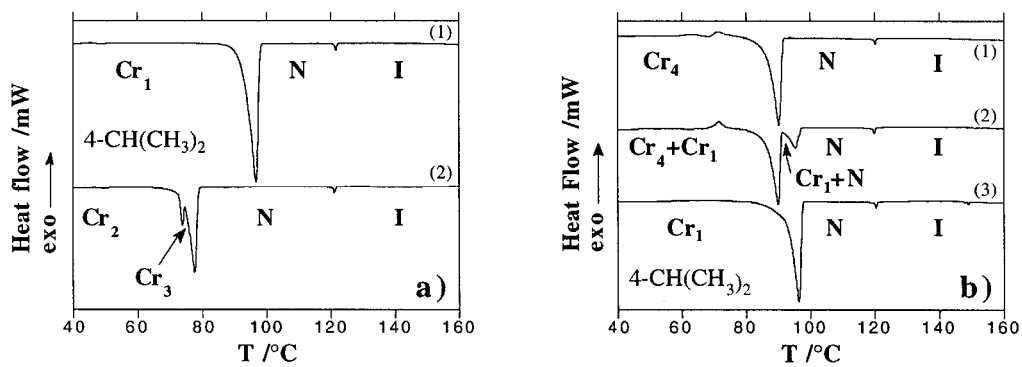

Figure 3. Successive thermograms of **4-CH(CH$_3$)$_2$**. (*a*) Upper, unmelted compound; lower, melted compound. (*b*) The sample was subjected to different thermal treatments (see text) before the thermograms were recorded.

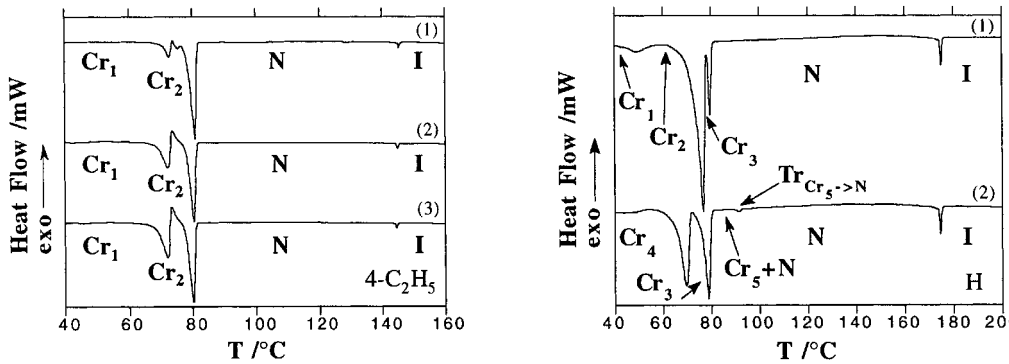

Figure 4. Successive thermograms of compounds **4-C_2H_5** (left) and **H** (right). The temperature cycling was a heating step: 35–200°C, then a cooling step: 200–35°C with a heating/cooling rate of 10°C min^{-1} and a 30 min hold at 35°C before the next cycle.

history of the compound. Microscopic observation, after melting and cooling the sample, showed that this solid crystallized in needles (Cr_2). If the second heating process is stopped at 82°C when the Cr_3 form has melted into the nematic phase, a new (button shaped) solid (Cr_4) crystallizes very slowly in the nematic phase. This solid melts into the nematic phase on further heating to 91°C. If the heating is stopped at 94°C, Cr_1 solid grows in the nematic phase as nice prisms. This solid melts at 97°C, the same temperature as that for the unmelted compound. Cr_1 is the last solid obtained in the cycling process, therefore it is the thermodynamically stable crystalline phase. This behaviour is further illustrated in figure 3(*b*). The sample was heated above the clearing temperature, then cooled at 15°C min^{-1}, and left at 35°C for 30 min. Then, the sample was heated to 82°C and left at this temperature for 30 min (longer periods gave the same DSC curve). The sample was then cooled to 35°C, and the thermogram was recorded with a heating rate of 5°C min^{-1} up to the clearing point. The thermogram in figure 3(*b*,1) shows the same melting temperature at 91°C, which is evidence for the formation of solid Cr_4. In a second thermal treatment, the sample was similarly treated, but was left at 82°C for only 1 min instead of 30 min before cooling to 35°C (and left at this temperature for 1 h). The thermogram, figure 3(*b*,2), shows two solid–nematic transitions, one at 91°C and the second at 97°C, indicating that Cr_4 and Cr_1 solids were obtained simultaneously by this particular thermal treatment. When this sample was left overnight at 35°C instead of 1 h, the Cr_4 solid was completely converted into Cr_1, figure 3(*b*,3).

The compound **4-C_2H_5** exhibits a different behaviour, figure 4(*a*). In the solid phase, four peaks were observed in the thermogram during the first heating; three are endothermic and one is slightly exothermic. During the second heating, the smallest endothermic peak disappeared, and the exothermic peak became more intense. The maxima of the remaining peaks appear at the same temperature, but the intensity of the first endothermic peak increased slowly on further cycles; from top to bottom in figure 4(*a*). The conversion into the solid phases can be followed optically. When we left the compound at 40°C for 1 h, a nicely crystallized sample was obtained. When we heated this film at 73.5°C (maximum of the exothermic peak), there was a structural change in the film corresponding to the solid stable at high temperature. Many cracks appear in the sample: obviously Cr_2 is more dense than Cr_1. The exothermic peak is probably induced by some structural changes in the conformation of the lateral substituent.

In figure 4(*b*), two thermograms of the compound **H** are presented for the unmelted and melted material. Obviously, after melting the original sample, new solid phases were formed. Under microscopic examination, a clear solid–solid transition was observed at 70°C corresponding to the first transition, giving the solid Cr_3 which melts at 79°C to give the nematic phase. When the temperature was kept constant at 84°C, a new solid appeared. This solid grew into the nematic phase as platelets which melted at 91.5°C, corresponding to the small final peak in the DSC trace. As shown on the thermogram, the solid Cr_5 appears on cooling, but it is kinetically unfavourable.

3.3. *Chemical shift changes of the aromatic rings*

Figures 5(*a*) and 5(*b*) show the ^{13}C NMR spectra of the phenyl carbons in **4-CH_3** in the mixture ZLI 1167-**4-CH_3**. In the nematic phase, 5(*b*), all the aromatic peaks show large changes in the chemical shifts compared with those in the isotropic phase, 5(*a*). Changes in the quaternary carbons usually are the largest due to the particular position of the *para*-axes with respect to the frame of the chemical shift tensor, especially the carboxy (Ca and Cb) carbons and the phenyl carbons along the *para*-axis in the phenyl rings of the core (C1, C4, C5, and C8).

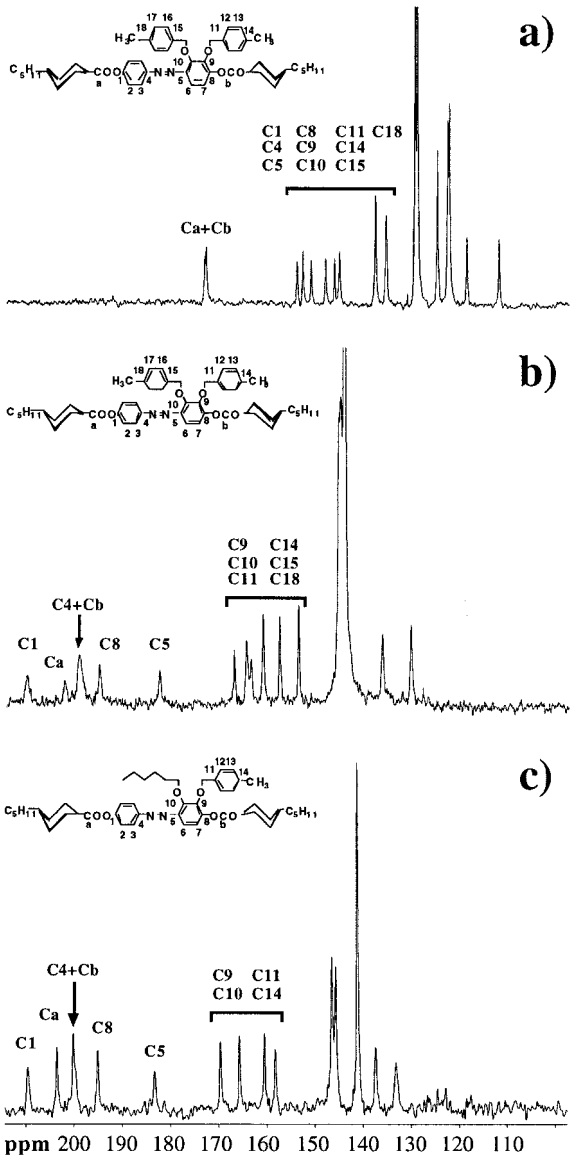

Figure 5. Aromatic chemical shifts in **4-CH$_3$** in the isotropic phase (*a*) and comparison of the anisotropic chemical shifts in **4-CH$_3$** (*b*) and in **4-CH$_3$-C6NN** (*c*) at the same reduced temperature ($T/T_{NI} = 0.94$).

When the anisotropic spectrum is compared with that of pure **4-CH$_3$-C6NN** at the same reduced temperature, figure 5(*c*), the features are essentially the same, except for the peaks of the second lateral phenyl ring (C15 and C18 are resolved, and C16 and C17 are not resolved).

In the compounds **4-CH$_3$-C6NN** and **4-CH$_3$-C6COO**, it was shown that the *para*-axes of the phenyl rings of the core nearly align with the molecular long axis and are not very dependent on the relative position of the lateral chain and the lateral ring [17]. Judging from the identical positions of C1 and C4 peaks shown in figures 5(*b*) and 5(*c*), we can assert that the replacement of a lateral chain by a second lateral aromatic ring does not appreciably modify the relative position of the molecular long axis. Thus, the *para*-axis of the ring bearing C1 and C2 in **4-CH$_3$** also aligns with the long core molecular axis.

The two new peaks appearing in the 150–170 ppm region are attributed to the quaternary carbons C15 and C18. Comparing the chemical shifts of all the peaks in figures 5(*b*) and 5(*c*), it can be seen that the four quaternary carbons (C11, C14, C15 and C18) belonging to the lateral aromatic rings have much smaller anisotropy than C1 and C4, but have anisotropies similar to those of C9 and C10, which are the quaternary carbons not placed on the molecular long axis. This indicates that the order parameters S_{zz} for the lateral rings are small due to the tilt of the *para*-axis in the lateral branch.

Some molecular dynamics calculations (using Nemesis 2.0 program) were performed for a single molecule in order to obtain information about the steric hindrance between the two lateral branches. The results are given in figure 6, which shows that one lateral aromatic branch is below the mean plane to which it is attached, while the other is above that plane. This molecular arrangement is possible due to the *gauche*-conformation of the first fragment. The two *para*-axes of the lateral rings are close to the magic angle with respect to the molecular long axis.

4. Conclusion

New nematic compounds deviating from the classical rod-like shape have been synthesized. They contain four rings in the main core and two nearby, lateral, substituted benzyloxy groups. They exhibit a wide nematic range which decreases with the bulkiness of the *para*-substituent of the lateral benzyloxy branches; if the lateral branch is substituted in the *ortho*- or *meta*-position, the melting temperatures decrease with a small effect on the nematic range. These compounds exhibit a rich solid polymorphism. Several solids with different melting temperatures can be obtained depending on the thermal

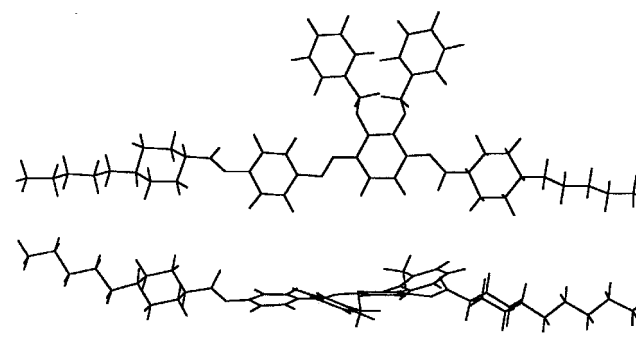

Figure 6. Minimized molecular conformation in compound **H** using Nemesis program.

history of the sample. ^{13}C NMR spectra indicate that the *para*-axis of the aromatic ring in the lateral branch makes a considerable angle with the core. Molecular modelling asserts this particular geometry, and shows that this angle is near the magic angle with respect to the *para*-axis.

The work of B.M.F. was supported by the US National Science Foundation under grant number DMR-9700680.

References

[1] Gray, G. W., 1974, *Liquid Crystals and Plastic Crystals* (Chichester: Ellis Horwood).
[2] Toyne, K. J., 1987, *Thermotropic Liquid Crystals* (Chichester: John Wiley).
[3] Osman, M. A., 1985, *Mol. Cryst. liq. Cryst.*, **128,** 45.
[4] Hasegawa, H., Matsunaga, Y., and Miyajima, N., 1991, *Bull. chem. Soc. Jpn.*, **64,** 296.
[5] Perez, F., Judeinstein, P., Bayle, J.-P., Allouchi, H., Cotrait, M., and Lafontaine, E., 1996, *Liq. Cryst.*, **21,** 855.
[6] Perez, F., Bayle, J.-P., and Fung, B. M., 1996, *New. J. Chem.*, **20,** 537.
[7] Perez, F., Judeinstein, P., Bayle, J.-P., Roussel, F., and Fung, B. M., 1997, *Liq. Cryst.*, **22,** 711.
[8] Norbert, W. D. J. A., Goodby, J. W., Hird, M., and Toyne, K. J., 1997, *Liq. Cryst.*, **22,** 631.
[9] Weissflog, W., and Demus, D., 1983, *Cryst. Res. Tech.*, **18,** K21.
[10] Weissflog, W., and Demus, D., 1984, *Cryst. Res. Tech.*, **19,** 55.
[11] Weissflog, W., and Demus, D., 1985, *Mol. Cryst. liq. Cryst.*, **129,** 235.
[12] Imrie, C. T., and Taylor, L., 1989, *Liq. Cryst.*, **6,** 1.
[13] Bezborodov, V. S., and Petrov, V. F., 1997, *Liq. Cryst.*, **23,** 771.
[14] Attard, G. S., and Imrie, C. T., 1989, *Liq. Cryst.*, **6,** 387.
[15] Berdaguè, P., Perez, F., Bayle, J.-P., Ho, M. S., and Fung, B. M., 1995, *New. J. Chem.*, **19,** 383.
[16] Berdaguè, P., Perez, F., Judeinstein, P., and Bayle, J.-P., 1995, *New. J. Chem.*, **19,** 293.
[17] Perez, F., Judeinstein, P., Bayle, J.-P., Allouchi, H., Cotrait, M., Roussel, F., and Fung, B. M., 1998, *Liq. Cryst.*, **24,** 627.
[18] Chandrasekhar, S., Nair, G., Shankar Rao, D. S., Krishna Rasad, S., Praefcke, K., and Blunk, D., 1998, *Liq. Cryst.*, **24,** 67.